

# Phase diagram and local tunneling spectroscopy of the Fulde-Ferrell-Larkin-Ovchinnikov states of a two-dimensional square-lattice $d$ -wave superconductor

Tao Zhou and C. S. Ting

*Texas Center for Superconductivity and Department of Physics, University of Houston, Houston, Texas 77204, USA*  
(Received 11 June 2009; revised manuscript received 18 November 2009; published 17 December 2009)

We studied the phase diagram for a two-dimensional square-lattice  $d$ -wave superconducting system under an exchange field. According to the spatial configuration of the order parameter, we show that the  $H$ - $T$  phase diagram should include the uniform phase, the one-dimensional Fulde-Ferrell-Larkin-Ovchinnikov (FFLO) state, and the two-dimensional FFLO state. The local density of states are calculated and suggested to be signatures to distinguish these phases.

DOI: [10.1103/PhysRevB.80.224515](https://doi.org/10.1103/PhysRevB.80.224515)

PACS number(s): 74.20.Fg, 74.25.Dw, 74.81.-g

The Fulde-Ferrell-Larkin-Ovchinnikov (FFLO) state was predicted several decades ago by Fulde and Ferrell (FF) (Ref. 1) and Larkin and Ovchinnikov (LO) (Ref. 2) for the superconductor in a strong magnetic field, where the superconducting (SC) order parameter varies periodically in space. While the occurrence of the FFLO state requires very stringent conditions on the SC materials, namely, the Pauli paramagnetism effect should dominate over the orbital effect,<sup>3</sup> and the material needs to be very clean.<sup>4</sup> As a result, this long thought of inhomogeneous SC state has never been observed in conventional superconductors.

For layered systems with an exchange field or a magnetic field parallel to the SC plane, the orbital effect will be suppressed strongly due to the low dimensionality. Thus they could be strong candidates to look for the FFLO state. Actually, in the past decade, indications for possible FFLO state have been reported in the heavy fermion materials CeCoIn<sub>5</sub>,<sup>5-7</sup> organic superconductors  $\lambda$ -(BETS)<sub>2</sub>GaCl<sub>4</sub>,<sup>8</sup>  $\lambda$ -(BETS)<sub>2</sub>FeCl<sub>4</sub>,<sup>9,10</sup> and  $\kappa$ -(BEDT-TTF)<sub>2</sub>Cu(NCS)<sub>2</sub>.<sup>11,12</sup> All of them are quasi-two-dimensional (2D) layered compounds. The experimental developments have attracted renewed interest on the property of the FFLO state. Theoretically, the existence and the character of the FFLO state can be investigated through analyzing the free-energy function of different gap structures. Alternatively, one can obtain the order parameter self-consistently based on the Bogoliubov-de-Gennes (BdG) technique or Eilenberger equation. In fact, in the past, the FFLO state has been studied intensively based on the above techniques.<sup>13-26</sup> One intriguing question is the detailed gap structure in the FFLO state. Up to now it is still an open question and different groups have claimed different results. For a 2D isotropic system and  $s$ -wave pairing symmetry, different periodic gap structures, i.e., one-dimensional (1D) FF state ( $\Delta \sim e^{iqr}$ ), 1D LO state [ $\Delta \sim \cos(qr)$ ], and 2D states with square state, triangular state, and hexagonal state, were proposed in Ref. 16. In their calculation, the gap structure depended on the temperature and the 2D structure was favored over the 1D structure at high magnetic field and low temperature. Later, Mora, and Combescot proposed that the gap structure could be written as the superposition of the plane waves with the number of the plane waves tending to be infinity as the temperature tended to be zero.<sup>17</sup> A recent paper plotted the  $H$ - $T$  phase diagram for the 2D isotropic

systems. The 1D FFLO state and 2D FFLO states with square, triangular, and hexagonal patterns were shown in the diagram, where the structure transition in their results was induced by the exchange field  $H$ . While the structure they obtained depended weakly on the temperature  $T$ .<sup>18</sup> On the other hand, for a  $d$ -wave pairing symmetry, Ref. 16 suggested that the 2D gap structure was favored at high magnetic field and low temperature. It was also stated in Ref. 19 that the 2D gap structure was the only stable solution in  $d$ -wave pairing symmetry superconductors. However, it was proposed that the phase diagram included different 1D stripe states with the orientations of the stripe along parallel and diagonal directions, respectively.<sup>15</sup> For the crystal system with square lattice, based on the BdG technique, a 1D stripe-like pattern for  $s$ -wave pairing symmetry was proposed.<sup>21,22</sup> For 2D  $d$ -wave superconductors, it was proposed<sup>21</sup> that the order parameter had a 2D checkerboard pattern. Furthermore, in the presence of dilute impurities, the pattern of the FFLO state became 1D stripelike in a 2D  $d$ -wave superconductor.<sup>25,26</sup> This implies that the 2D and 1D FFLO states may be present in the 2D square-lattice system in different parameter region.

Summing up all the previous theoretical results, the gap structure of the 2D superconductors is still unclear, for both isotropic superconductors and lattice systems, for both  $s$ -wave and  $d$ -wave pairing symmetries. The calculations based on the lattice model are relatively less while on the other hand, the FFLO states are most possible to occur in the lattice system (e.g., CeCoIn<sub>5</sub> and certain organic superconductors). Up to now, a systematic investigation for the gap structure in the 2D  $d$ -wave square-lattice system is still lacking. The motivation of the present work is to fill this void and calculate the spatially distributed order parameter self-consistently based on the BdG equations on a 2D  $d$ -wave square lattice. The whole  $H$ - $T$  phase diagram is constructed. We verify numerically that the gap structure in the FFLO state for 2D  $d$ -wave square-lattice samples is not always simply 2D. Previous calculations based on BdG technique<sup>21,25</sup> focus on higher exchange field, thus an additional region, i.e., 1D FFLO state was omitted. At zero temperature, the pattern changes from the uniform state to the 1D FFLO state and then to the 2D FFLO state as the strength of the exchange field increases. The periodicity of the 1D and 2D FFLO states decreases as the exchange field increases. At

finite temperature, the 1D FFLO state will transit to the uniform phase upon increasing the temperature. Thus near the SC transition temperature, only uniform phase and 2D FFLO state are observed. The local density of states (LDOS) for the above states are also calculated and they provide definitive signatures for the above-mentioned FFLO states. In addition, our numerical study indicates that for a 2D  $s$ -wave superconductor in the square lattice, the FFLO state is always 1D like and no 2D pattern could be obtained, this conclusion is consistent with that of Refs. 21 and 22 and the result will not be presented here.

We start from a phenomenological tight-binding model with the Zeeman splitting effect caused by an exchange field or in-plane magnetic field. On a two-dimensional square lattice with a pairing interaction  $V$  between the nearest-neighbor sites, the mean-field Hamiltonian leading to the  $d$ -wave superconductivity can be written as

$$H = - \sum_{ij\sigma} (t_{ij} c_{i\sigma}^\dagger c_{j\sigma} + \text{H.c.}) - \sum_{i\sigma} (\mu + \sigma h) c_{i\sigma}^\dagger c_{i\sigma} + \sum_{ij} (\Delta_{ij} c_{i\uparrow}^\dagger c_{j\downarrow}^\dagger + \text{H.c.}), \quad (1)$$

where  $t_{ij}$  are the hopping constants and  $\mu$  is the chemical potential.  $\sigma h = \sigma g \mu_B H$  ( $g$  and  $\mu_B$  are the Lande factor and Bohr magneton, respectively) is the Zeeman energy term, caused by the interaction between the magnetic field and the spins, with  $\sigma = \pm 1$  representing for spin-up and spin-down electrons, respectively. The orbital effect, (which is suggested to exist in layered compounds  $\text{CeInO}_5$  by Ref. 27) is neglected here. The SC order parameter has the following definition:  $\Delta_{ij} = V \langle c_{i\uparrow} c_{j\downarrow} - c_{i\downarrow} c_{j\uparrow} \rangle / 2$ .

This Hamiltonian can be diagonalized by solving the BdG equations,

$$\sum_j \begin{pmatrix} H_{ij} & \Delta_{ij} \\ \Delta_{ij}^* & -H_{ij}^* \end{pmatrix} \begin{pmatrix} u_{j\uparrow}^n \\ v_{j\downarrow}^n \end{pmatrix} = E_n \begin{pmatrix} u_{i\uparrow}^n \\ v_{i\downarrow}^n \end{pmatrix}, \quad (2)$$

where  $H_{ij}$  is expressed by

$$H_{ij} = -t_{ij} - (\mu + \sigma h) \delta_{ij}. \quad (3)$$

The SC order parameter and the local electron density  $n_i$  satisfy the following self-consistent conditions:

$$\Delta_{ij} = \frac{V_{ij}}{4} \sum_n (u_{i\uparrow}^n v_{j\downarrow}^{n*} + u_{j\uparrow}^n v_{i\downarrow}^{n*}) \tanh\left(\frac{E_n}{2K_B T}\right), \quad (4)$$

$$n_i = \sum_n |u_{i\uparrow}^n|^2 f(E_n) + \sum_n |v_{i\downarrow}^n|^2 [1 - f(E_n)]. \quad (5)$$

Here  $f(x)$  is the Fermi distribution function.

In a self-consistent calculation, the BdG equations [Eq. (2)] are diagonalized with a set of random distributed initial values of the order parameter  $\Delta_{ij}$  and the on-site electron density  $n(i)$ . The new values of  $\Delta_{ij}$  and  $n(i)$  are calculated from Eqs. (4) and (5) and used as input parameters for the next iteration step. Such procedure is repeated until the desired convergence criterion is satisfied. For the nearest-neighbor attracted interaction we adopted, both extended  $s$ -wave and  $d_{x^2-y^2}$ -wave pairing symmetries are possible stable solutions. Which solution is more favorable may de-

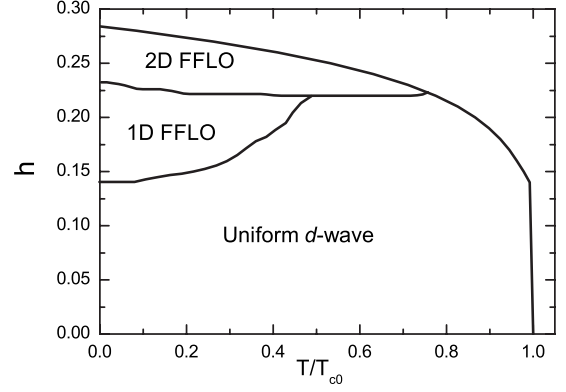


FIG. 1.  $H$ - $T$  phase diagram of the two-dimensional  $d$ -wave superconductor in the parallel magnetic field.  $h = g \mu_B H$  is the exchange field.  $T_{c0} \approx 0.19$  is the SC transition temperature in zero field.

pend on the band structure. In the present work, we have carried out extensive calculations with different initial values of the input parameters. The order parameters we obtained have always the same magnitude and opposite signs along  $x$  direction and  $y$  direction, corresponding to the  $d_{x^2-y^2}$ -wave pairing symmetry. We define the magnetization  $m_i$  and the  $d$ -wave SC order parameter  $\Delta_i$  as  $m_i = \langle S^z \rangle = (\hbar/2) \langle n_{i\uparrow} - n_{i\downarrow} \rangle$  and  $\Delta_i = 1/4 (\Delta_{i,i+\hat{x}} + \Delta_{i,i-\hat{x}} - \Delta_{i,i+\hat{y}} - \Delta_{i,i-\hat{y}})$ .

The LDOS is expressed by

$$\rho_i(\omega) = \sum_n [ |u_{i\uparrow}^n|^2 \delta(E_n - \omega) + |v_{i\downarrow}^n|^2 \delta(E_n + \omega) ], \quad (6)$$

where the delta function  $\delta(x)$  is taken as  $\Gamma / \pi(x^2 + \Gamma^2)$  with  $\Gamma = 0.01$ . The supercell technical is used to calculate the LDOS.

In the following calculation, we take the hopping constant  $t_{ij}$  to be unity for nearest neighbors and zero otherwise. The pairing potential  $V$  and the filling electron density  $n$  are chosen as  $V = 1.3$  and  $n = 0.84$  (hole-doped samples with doping  $\delta = 0.16$ ), respectively. The calculation is made on  $48 \times 48$  lattice with periodic boundary condition and random distributed initial values of the order parameters are chosen. The  $10 \times 10$  supercell is used to calculate the LDOS.

Before presenting our results, it is important to point out the limitations of the present model. The finite-size effect constrains our results are effective only when the exchange field is not too weak. Some of solutions are perhaps not obtained due to the finite-size effect and the periodic boundary condition we adopted. We also stress that the results we obtained is not necessarily the same with those based on the continuum model, although we wish that our calculations could be complementary to existing continuum model studies.

We summarize our main results in Fig. 1, as seen, the  $H$ - $T$  phase diagram is plotted. At zero temperatures two critical Zeeman fields  $h_1 = 0.14$  and  $h_2 = 0.23$ , are revealed. The whole SC state is divided to be three regions, namely, uniform  $d$ -wave SC state, 1D FFLO state, and 2D FFLO state, respectively. The periodicity will decrease as the magnetic field increases in both 1D and 2D FFLO states. As  $h > 0.28$ ,

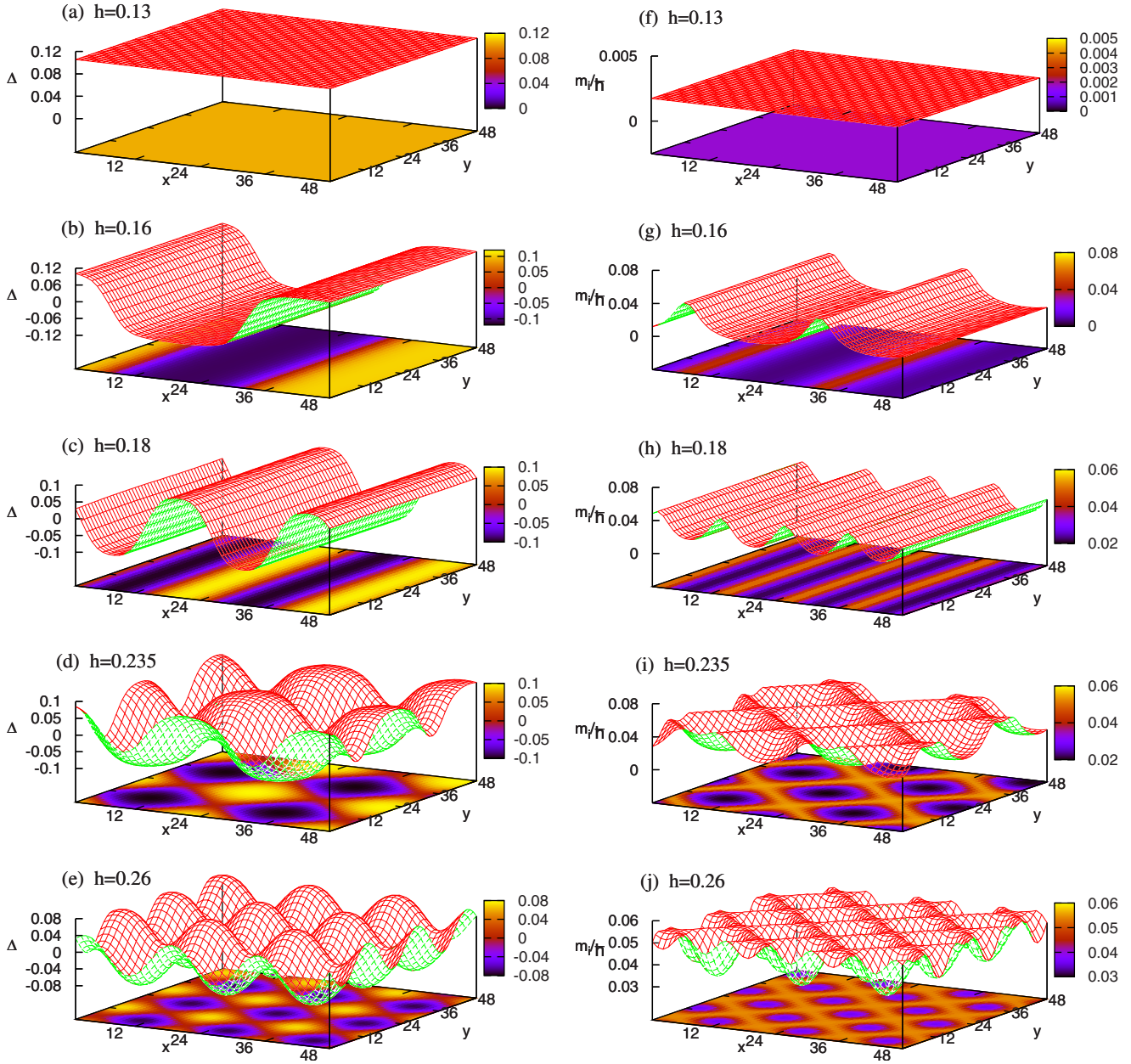


FIG. 2. (Color online) Plots of the order parameter  $\Delta$  (left panels) and the magnetization  $m_i$  (right panels) as a function of position for various Zeeman fields  $h$  with  $T=10^{-5}$ .

the SC phase will be destroyed completely. The periodicity of the 1D FFLO state also increases as the temperature increases, and it will transit to the uniform state as the temperature increases further. As a result, the range of the FFLO phase will decrease upon increasing the temperature. Near the SC transition temperature, only uniform  $d$ -wave phase and 2D FFLO phase were observed, with the transition field at about  $h=0.225$ .

The calculated order-parameter amplitudes and the magnetization for various Zeeman fields  $h$  with the temperature  $T=10^{-5}$  are shown in Figs. 2(a)–2(j). The order parameters are plotted in left panels. As seen, for weaker magnetic field, the order parameter is uniform [Fig. 2(a)]. The magnitude of the order parameter  $\Delta_0$  equals to 0.106 at zero field. It depends weakly on  $h$  at low fields and equals to 0.1056 as  $h$

$=0.13$  [Fig. 2(a)]. When the Zeeman field increases further, as we can see from Figs. 2(b) and 2(c), the SC order forms the stripe pattern. The order parameter is of nearly cosine form with the periodicity of about 48 along  $x$  direction as  $h=0.16$ . We have verified numerically that the periodicity is kept to be 48 for  $0.14 < h < 0.175$ . And the periodicity reduces to 24 as  $h$  increases ( $0.175 < h < 0.23$ ). Here the finite-size effect prevents us from obtaining solutions with periodicity not commensurate with the lattice size. As  $h$  increases further, the pattern changes to two dimensional and a supersquare-lattice forms, with the periodicity decreases as  $h$  increases, which can be seen clearly from Figs. 2(d) and 2(e).

The spatial distributions of the magnetization (with the units  $\hbar$ ) are shown in Figs. 2(f)–2(j). As seen in Fig. 2(f), in the uniform phase, the distribution is also uniform. The mag-

netization is suppressed strongly by the SC order, as a result, it is quite weak ( $\approx 0.0015$ ) for small exchange field ( $h=0.13$ ). We also checked numerically (not presented here) that the magnitude will increase to about 0.025 in the normal state for the same magnetic field ( $h=0.13$ ). In the 1D FFLO state, as seen in Figs. 2(g) and 2(h), the intensity is largest along the nodal lines and is suppressed when the SC order parameter increases. It reaches the minimum value as the SC order is maximum. The pattern also forms 1D stripe but the periodicity is one half of that of the order parameter. In the 2D FFLO state [Figs. 2(i) and 2(j)], the structure of the magnetization forms the checkerboard pattern. Similar to the case of 1D FFLO state, the intensity of magnetization is largest at the nodal lines and minimum as the SC order is maximum. The periodicity along the parallel direction is the same as that of the order parameter. While the periodicity along the diagonal direction is only one half of that of the order parameter.

Our results of the phase diagram and order-parameter structure shown in Figs. 1 and 2 are different with previous analytic calculations on both  $d$ -wave and  $s$ -wave 2D isotropic superconductors.<sup>13–19</sup> For instance, based on the continuum model and taking into account the  $d$ -wave pairing symmetry, it was proposed that the FFLO momentum could change from 0 to  $\pm\pi/4$ , dependent on the exchange field and the temperature.<sup>13–15</sup> In real space, the different FFLO momentum corresponds to the different orientations of the stripes or supersquare lattice in the FFLO state. However, our present results are significantly different, i.e., the smallest periods of the order parameter are always along the unit-cell direction for both 1D FFLO state and 2D FFLO state, independent of the temperature and the exchange field. On the other hand, our results also show some similarities with those based on the continuum model, e.g., at higher temperature near the SC transition temperature, the results are somewhat consistent with Maki and Won's calculation,<sup>19</sup> i.e., the prime FFLO state has 2D structure, no 1D state was observed. At low temperature, the results are somewhat consistent with the recent proposed phase diagram,<sup>18</sup> namely, the energy favored state transforms from the uniform state to 1D FFLO state then to 2D FFLO state as the exchange field increases. However, here no triangle and hexagonal states were obtained. The absence of these two states is due to the system's symmetry. In fact, the phase transition in condensed-matter physics will relate to the symmetry breaking. The order parameter is a description of the lowered symmetry in the ordered state. The symmetry group describing the SC state must be a subgroup of the full symmetry group  $G$  describing the normal state,<sup>28</sup>

$$G = X \times R \times U(1) \times T, \quad (7)$$

where  $X$  is the symmetry group of the crystal lattice,  $R$  is the symmetry group of spin rotation,  $U(1)$  is the one-dimensional global gauge symmetry, and  $T$  is the time-reversal symmetry operation. For the square lattice, the symmetry group of the crystal lattice should have the point-group symmetry with  $D_{4h}$ . The spin-rotation symmetry  $R$  will be broken by the exchange field. The symmetry groups of both 1D FFLO state and 2D FFLO state with square superlattice

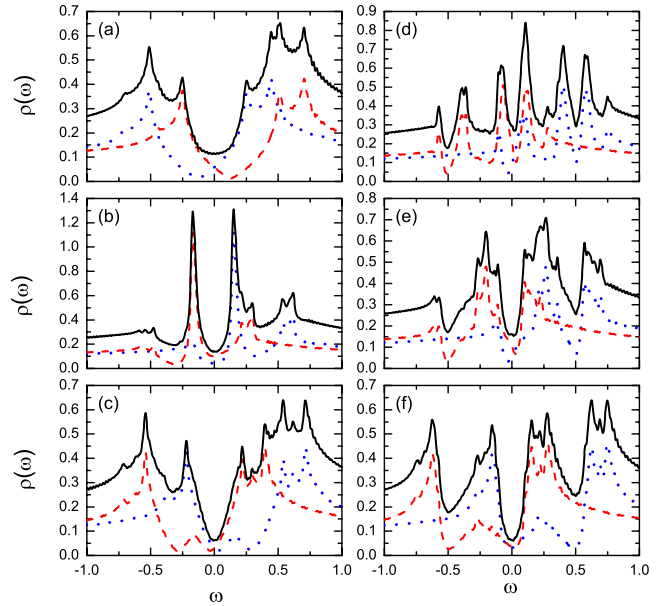


FIG. 3. (Color online) The LDOS spectra for different phases. Panel (a) is the LDOS in the uniform phase with  $h=0.13$ . Panels (b) and (c) are the spectra in the 1D FFLO phase with  $h=0.16$  at the nodal line and at the site where the order parameter is maximum, respectively. The right panels are the spectra in the 2D FFLO phase with  $h=0.235$ , where (d)–(f) are the spectra at the saddle point where two nodal lines intersect, the midsite between two neighboring saddle points, and the site where the order parameter has the maximum magnitude, respectively. The (blue) dotted line, (red) dashed line, and the (black) solid line are spin-up LDOS, spin-down LDOS, and whole LDOS, respectively.

are subgroups of  $D_{4h}$ , thus these two states can survive for the square crystal lattice. However, the 2D FFLO states with triangle and hexagonal superlattice contain the symmetry operator which are not belong to the  $D_{4h}$  group, as a result, they could not exist in the square crystal lattice. While on the other hand, they may exist in triangle crystal lattice and hexagonal crystal lattice, respectively. A systematic comparison for the differences and similarities of the FFLO states in lattice systems and isotropic systems with different pairing symmetries still needs further study. Here we will focus on discussing the property of the obtained states.

We now turn to study the LDOS spectra. The LDOS [Eq. (6)] can be written as  $\rho_i = \rho_{i\uparrow} + \rho_{i\downarrow}$ . Here  $\rho_{i\uparrow}$  and  $\rho_{i\downarrow}$  are, respectively, the spin-up and spin-down parts of the LDOS. These two parts are exactly the same if the Zeeman field is absent. In presence of the Zeeman field, the spin-up LDOS shifts to left and the spin-down LDOS shifts to right. In Figs. 3(a)–3(f), we plot the two parts of LDOS separately to discuss the properties of the LDOS. The whole LDOS spectra are also plotted so that the results can be compared with scanning tunneling microscopy (STM) experiments.

The LDOS spectra in the uniform phase are shown in Fig. 3(a). As seen, the spin-up LDOS shifts to the left with the midgap point locating at  $\omega = -h$ . The SC coherent peaks shift to  $\pm\Delta_0 - h$ . The spin-down LDOS shifts to the right with the SC coherent peaks at  $\pm\Delta_0 + h$ . Outside the gap we can see the Van Hove peak. As a result, the whole LDOS spectrum

contains two stronger peaks at  $\pm(\Delta_0+h)$  and two weaker peaks at  $\pm(\Delta_0-h)$ . The gap structure at low energies is “U” shaped. The density of states at zero energy  $\rho(0)$  increases linear with the external field, indicating the quasiparticle excitations due to the magnetic fields.

The LDOS spectra in the 1D FFLO phase with  $h=0.16$  are shown in Figs. 3(b) and 3(c). Figure 3(b) is for the site on the nodal line. We can see very sharp and strong peaks at the position  $\pm h$ . The SC coherent peaks are suppressed and almost invisible. The peak at negative energy comes from the spin-up LDOS and the peak at positive energy are contributed by the spin-down LDOS. Taking into account the Zeeman shift, these in-gap peaks (bound states) at  $\pm h$  locate just at the midgap position. These bound states are due to the sign change in the order parameter across the nodal lines and are related to the Andreev reflections, similar to the midgap states in *d*-wave superconductors.<sup>29</sup> The intensity of the in-gap peaks will decrease as the site moves away from the nodal line. As we can see from Fig. 3(c), at the site where the order parameter is maximum, the in-gap peaks are turned to be a hump at the midgap position for both spin-up and spin-down LDOS spectra. The SC coherent peaks are seen clearly. The midgap hump is so weak that it is concealed in the whole LDOS ( $\rho_i$ ) spectrum. We can see four peaks at the energies  $[\pm(\Delta_0 \pm h)]$ . And the spectrum of the whole LDOS is similar to that of the uniform phase while the gap structure at low energies is not U shaped but “V” shaped due to the presence of the midgap hump.

At last we plot the LDOS spectra of the 2D FFLO phase in Figs. 3(d)–3(f). Actually the features of the spin-up LDOS spectra are studied intensively in Ref. 21. There are two kinds of Andreev bound states. One is due to the sign change in the order parameter across the nodal lines. The second is essentially localized at the saddle points. The order parameter is suppressed strongly in an intersecting region, which

produces a potential well for a quasiparticle and thus generates two finite-energy Andreev bound states. As a result, at the saddle points, four in-gap peaks exist in the spin-up LDOS spectra [Fig. 3(d)] at the energies  $-0.575$ ,  $-0.385$ ,  $-0.08$ , and  $0.105$ . And midgap peaks exist between two neighboring saddle points [Fig. 3(e)]. At the site where the order parameter is maximum, the LDOS spectrum [Fig. 3(f)] is similar to that of the 1D FFLO state [Fig. 3(b)] and that of the uniform phase, namely, if the Van hove peaks and the weak peak caused by the midgap hump are excluded, there are only four peaks left, locating at  $\pm(\Delta_0 \pm h)$ , contributed by the spin-up and spin-down LDOS, respectively.

We have shown the LDOS spectra of the three different phases. As seen in Figs. 3(a)–3(f), the spectra are quite different and the spectra in each phase have their distinctive features as we discussed above. Thus they can be easily detected by the STM experiments and can be used as signatures to probe the FFLO states.

In summary, based on a BCS-type model and BdG equations, we studied the phase diagram and the order-parameter structure in presence of the external exchange field. The phase diagram is mapped out and it includes the regions of uniform phase, 1D FFLO state, and 2D FFLO state, respectively. We also calculate the LDOS to discuss the signatures of the three phases, namely, the LDOS spectra in the uniform phase will contain four peaks due to the Zeeman shift. In the 1D FFLO state, the LDOS spectra show midgap states due to the Andreev reflection. In the 2D FFLO states, four in-gap peaks are revealed at the saddle point due to two kinds of Andreev bound states. Thus in each states the LDOS has its unique feature and may be used as powerful tools to distinguish these states.

This work was supported by the Texas Center for Superconductivity at the University of Houston and by the Robert A. Welch Foundation under the Grant No. E-1146.

<sup>1</sup>P. Fulde and R. A. Ferrell, Phys. Rev. **135**, A550 (1964).

<sup>2</sup>A. I. Larkin and Yu. N. Ovchinnikov, Zh. Eksp. Teor. Fiz. **47**, 1136 (1964) [Sov. Phys. JETP **20**, 762 (1965)].

<sup>3</sup>L. W. Gruenberg and L. Gunther, Phys. Rev. Lett. **16**, 996 (1966).

<sup>4</sup>L. G. Aslamazov, Zh. Eksp. Teor. Fiz. **55**, 1477 (1968) [Sov. Phys. JETP **28**, 773 (1969)].

<sup>5</sup>H. A. Radovan, N. A. Fortune, T. P. Murphy, S. T. Hannahs, E. C. Palm, S. W. Tozer, and D. Hall, Nature (London) **425**, 51 (2003).

<sup>6</sup>A. Bianchi, R. Movshovich, C. Capan, P. G. Pagliuso, and J. L. Sarrao, Phys. Rev. Lett. **91**, 187004 (2003).

<sup>7</sup>K. Kumagai, M. Saitoh, T. Oyaizu, Y. Furukawa, S. Takashima, M. Nohara, H. Takagi, and Y. Matsuda, Phys. Rev. Lett. **97**, 227002 (2006).

<sup>8</sup>M. A. Tanatar, T. Ishiguro, H. Tanaka, and H. Kobayashi, Phys. Rev. B **66**, 134503 (2002).

<sup>9</sup>S. Uji, H. Shinagawa, T. Terashima, T. Yakabe, Y. Terai, M. Tokumoto, A. Kobayashi, H. Tanaka, and H. Kobayashi, Nature (London) **410**, 908 (2001).

<sup>10</sup>L. Balicas, J. S. Brooks, K. Storr, S. Uji, M. Tokumoto, H. Tanaka, H. Kobayashi, A. Kobayashi, V. Barzykin, and L. P. Gorkov, Phys. Rev. Lett. **87**, 067002 (2001).

<sup>11</sup>H. Shimahara, J. Phys. Soc. Jpn. **66**, 541 (1997).

<sup>12</sup>S. Manalo and U. Klein, J. Phys.: Condens. Matter **12**, L471 (2000).

<sup>13</sup>K. Maki and H. Won, Czech. J. Phys. **46**, 1035 (1996).

<sup>14</sup>K. Yang and S. L. Sondhi, Phys. Rev. B **57**, 8566 (1998).

<sup>15</sup>A. B. Vorontsov, J. A. Sauls, and M. J. Graf, Phys. Rev. B **72**, 184501 (2005).

<sup>16</sup>H. Shimahara, J. Phys. Soc. Jpn. **67**, 736 (1998).

<sup>17</sup>C. Mora and R. Combescot, Europhys. Lett. **66**, 833 (2004).

<sup>18</sup>Y. Matsuda and H. Shimahara, J. Phys. Soc. Jpn. **76**, 051005 (2007).

<sup>19</sup>K. Maki and H. Won, Physica B (Amsterdam) **322**, 315 (2002).

<sup>20</sup>R. Combescot and C. Mora, Phys. Rev. B **71**, 144517 (2005).

<sup>21</sup>Qian Wang, H.-Y. Chen, C.-R. Hu, and C. S. Ting, Phys. Rev. Lett. **96**, 117006 (2006).

<sup>22</sup>Q. Cui and K. Yang, Phys. Rev. B **78**, 054501 (2008).

<sup>23</sup>D. F. Agterberg and K. Yang, J. Phys.: Condens. Matter **13**, 9259

- (2001).
- <sup>24</sup>A. B. Vorontsov, I. Vekhter, and M. J. Graf, Phys. Rev. B **78**, 180505(R) (2008).
- <sup>25</sup>Q. Wang, C.-R. Hu, and C.-S. Ting, Phys. Rev. B **75**, 184515 (2007).
- <sup>26</sup>X.-J. Zuo and C.-D. Gong, EPL **86**, 47004 (2009).
- <sup>27</sup>Masanori Ichioka and Kazushige Machida, Phys. Rev. B **76**, 064502 (2007).
- <sup>28</sup>C. C. Tsuei and J. R. Kirtley, Rev. Mod. Phys. **72**, 969 (2000).
- <sup>29</sup>C.-R. Hu, Phys. Rev. Lett. **72**, 1526 (1994).